

Resilient Dynamic State Estimation for Multi-Machine Power System With Partial Missing Measurements

Yi Wang, *Member, IEEE*, Yaoqiang Wang, *Senior Member, IEEE*, Yonghui Sun, *Member, IEEE*, Venkata Dinavahi, *Fellow, IEEE*, Jun Liang, *Senior Member, IEEE*, and Kewen Wang, *Member, IEEE*

Abstract—Accurate tracking the dynamics of power system plays a significant role in its reliability, resilience and security. To achieve the reliable and precise estimation results, many advanced estimation methods have been developed. However, most of them are aiming at filtering the measurement noise, while the adverse affect of partial measurement missing is rarely taken into account. To deal with this issue, a discrete distribution in the interval [0,1] is introduced to depict mechanism of partial measurement data loss that caused by the sensor failure. Then, a resilient fault tolerant extended Kalman filter (FTEKF) is designed in the recursive filter framework. Eventually, extensive simulations are carried on the different scale test systems. Numerical experimental results illustrate that the resilience and robustness of the proposed fault tolerant EKF method against partial measurement data loss.

Index Terms—Sensor failure, partial missing measurements, extended Kalman filter, dynamic state estimation, power systems.

I. INTRODUCTION

STATE estimation is the key to various advanced applications in energy management systems (EMS), which can provide the paramount status information of the power system [1]-[3]. Generally speaking, the power system state estimation are composed of two categories, one of them is named static state estimation (SSE) and the other is called dynamic state estimation (DSE). Conventionally, the static states of power system at one time instant can be estimated by making use of a single set of redundant measurements [4]. However, the static state estimation cannot predict the future operation trend of system, which may not be sufficient for the analysis requirements of the power system with a high proportion of new energy sources [5]. Therefore, the DSE that is capable of capturing the dynamic changes in nonlinear power system has attracted much attention [6]-[7].

In this context, many different DSE approaches for power system have been developed. Among these numerous dynamic state estimation methods, Kalman filter (KF) and its variants are dominant due to their advantages in computational efficiency [6]-[16]. In [8], the feasibility of utilizing an extended Kalman filter (EKF) to track the dynamic states is investigated and confirmed. In [9], a decentralized EKF method that can estimate the unknown inputs and dynamic states simultaneously was developed. To enhance the robustness against disturbances, an iterated EKF was proposed in [10]. In addition, to alleviate the adverse impact of nonlinearity on DSE, by introducing the adaptive interpolation technique in the standard EKF, a multi-step method was proposed in [11]. Furthermore, several nonlinear filters were also developed and used to enhance the accuracy of DSE, such as the unscented Kalman filter (UKF) method that utilized the unscented transformation technique [12]-[15], the cubature Kalman filter (CKF) [16], [17], the ensemble Kalman filter (EnKF) [18], and the particle filter (PF) approach [19], [20].

These aforementioned works have greatly enhanced the monitoring level of power system, which can provide solid data information support for various advanced applications in the energy management system (EMS), such as the out-of-step detection for generators and the protection of series compensated transmission lines [21], [22], etc. However, it should be noted that most of the above methods are only aimed at filtering the measurement noise and improving the accuracy of DSE for power system under normal operating conditions, where

NOMENCLATURE

E_{fd}	Internal field voltage in p.u.
I_t	Terminal current phasor.
i_q, i_d	Currents in the q- and d-axes in p.u.
i_R, i_I	Real and imaginary of the terminal current phasor in p.u.
T_m	Mechanical torque in p.u.
T'_{d0}, T'_{q0}	Open-circuit time constants in the q- and d-axes in seconds.
S_B, S_N	System and generator base MVA.
P_e	Electrical active output power in p.u.
K_D	Damping factor in p.u.
Ψ	Voltage source vector.
Ψ_I, Ψ_R	Column vectors of all generators' imaginary and real parts of the voltage source on system reference frame.

This work was supported in part by the National Natural Science Foundation of China under Grant 62203395, in part by the Postdoctoral Research Project of Henan Province under Grant 202101011, and in part by the Key R&D and Promotion Project of Henan Province under Grant 222102220041. (Corresponding author: Yaoqiang Wang)

Yi Wang, Yaoqiang Wang, and Kewen Wang are with the School of Electrical and Information Engineering, Zhengzhou University, Zhengzhou 450001, China (e-mail: wangyi1414599008@163.com; wangyqee@163.com; kwwang@zzu.edu.cn).

Yonghui Sun is with the College of Energy and Electrical Engineering, Hohai University, Nanjing 210098, China (e-mail: sunyonghui168@gmail.com).

Venkata Dinavahi is with the Department of Electrical and Computer Engineering, University of Alberta, Edmonton, AB T6G 2V4, Canada (e-mail: dinavahi@ualberta.ca).

Jun Liang is with the School of Engineering, Cardiff University, Cardiff CF24 3AA, U.K. (e-mail: liangj1@cardiff.ac.uk).

the adverse affect that caused by inevitable measurements missing in the process of acquisition and transmission is rarely considered. Unfortunately, in the engineering practice, the measurements with intermittent information losses frequently occur due to the sensor malfunction or complex environments [23]. Thus, as verified in [24], the estimation performance of above discussed approaches may degrade seriously in the presence of incomplete measurement information.

To alleviate the adverse effects of measurement missing, meaningful research work has been carried out in [25]-[28]. Note that, in most of the existing literature, the measurement missing are often expressed by a random variable obeying Bernoulli distribution, where the measurements are assumed to be either utterly missing or completely available. However, for a practical power system, it is rare for the measurements to be completely lost, while the scenario of partial measurement data loss is relatively common [30]. For example, the data provided by phase measurement units (PMUs) are converted by the analog to digital converters (ADCs) from the continuous measurement signals; therefore, the output of ADCs may be subject to fading because of the poorly designed peripheral circuits or unstable reference voltage. In addition, the communication media such as the power lines and optical fiber channels may also attenuate the measurement signals [31]. The partial missing measurements phenomenon is quite distinct from the measurement data loss issue as discussed in the previous work [25]-[28], which should be re-examined. Therefore, how to model the partial missing measurements phenomenon in the DSE of power system and develop an resilient dynamic state estimator for power system is a challenging issue. This also constitutes the main motivation of our current research.

To deal with these challenges, in this paper, a resilient fault tolerant EKF that can suppress the adverse influence of partial measurement loss is designed. The main contributions of this paper are highlighted as follows:

- Firstly, the dynamic state estimation model of multi-machine power system with partial missing measurement is established;
- Secondly, a resilient fault tolerant extended Kalman filter is designed to deal with the adverse influence of partial measurements missing on the accuracy of dynamic state estimation for power system;
- Finally, the stability and convergence of the developed FTEKF approach are proved.

The rest of this paper is organized as follows. Section II establishes the DSE model of multi-machine power system with partial missing measurements. Section III develops the proposed resilient FTEKF approach. Section IV analyzes the numerical results on different test systems. Eventually, this paper is concluded in Section V.

Notation: The notation utilized here is comparatively standard unless otherwise stated. The subscript k represents the time instant. \hat{x}_k denotes the prior estimator of x_k , \hat{x}_k represents the posterior estimator of x_k . y_k indicates the measurement, I denotes the identity matrix. $E[\cdot]$ represents the expectation of the stochastic variable. \otimes indicates the Hadamard product, K_k represents the Kalman gain. Q_k means the covariance matrix of system noise, R_k denotes the

covariance matrix of measurement noise.

II. DYNAMIC MODEL OF MULTI-MACHINE POWER SYSTEM

In this part, the continuous dynamic model of power system that to track its states is established, which can be discretized by the modified Euler method [7]. More importantly, the phenomenon of partial missing measurements is fully analyzed and modeled in detail.

A. Continuous Model of Multi-Machine Power System

In this section, the synchronous generator and measurement model in [13] are applied to depict the dynamics of multi-machine power system, which allow both the fourth-order transient generator model and the second-order classical generator model.

For convenience of expression, let \mathcal{G}_2 and \mathcal{G}_4 respectively indicate the set of generators with second-order and fourth-order model in a power system. The number of generators with second-order or fourth-order model, which is also the cardinality of the sets \mathcal{G}_2 and \mathcal{G}_4 , are g_2 and g_4 , respectively. Therefore, the number of state variables to be estimated is $n = 2g_2 + 4g_4$. For generator $i \in \mathcal{G}_4$, the transient stability model of generator can be expressed by the fourth-order differential equations in local d - q reference frame:

$$\begin{cases} \dot{\delta}_i = \omega_i - \omega_0 \\ \dot{\omega}_i = \frac{\omega_0}{2H_i} \left(T_{mi} - T_{ei} - \frac{K_D}{\omega_0} (\omega_i - \omega_0) \right) \\ \dot{e}'_{qi} = \frac{1}{T'_{q0i}} (E_{fdi} - e'_{qi} - (x_{di} - x'_{di}) i_{di}) \\ \dot{e}'_{di} = \frac{1}{T'_{d0i}} (-e'_{di} + (x_{qi} - x'_{qi}) i_{qi}) \end{cases}, \quad (1)$$

where i indicates the generator serial number; δ , ω , e'_q and e'_d indicate the power angle, electrical angular velocity, transient electromotive force on q -axis and d -axis of a synchronous generator, respectively; ω_0 represents the initial value of ω ; K_D indicates the damping factor; T_j , T_m and T_e are respectively denote the inertia constant, mechanical and electromagnetic power; E_{fd} means the excitation voltage of stator; x_d , x'_d , x_q and x'_q are respectively symbolize the synchronous and transient reactance of generator's d -axis and q -axis; T'_{d0} , T'_{q0} , i_d and i_q indicate the d and q axis time constants and stator currents, respectively.

For the generator $i \in \mathcal{G}_2$, the classical generator model only contains the first two equations of (1), and the e'_{qi} and e'_{di} are kept unchanged; the state vector and the output vector are $\mathbf{x} = [\delta^T \ \omega^T]$ and $\mathbf{y} = [P_G^T \ Q_G^T \ V^T \ \theta^T]$, respectively.

To facilitate the notation, the continuous model of multi-machine power system expressed in (1) can be rewritten in a general state space form as follows

$$\begin{cases} \dot{\mathbf{x}} = \mathbf{f}_c(\mathbf{x}, \mathbf{u}) + \mathbf{w}_c \\ \mathbf{y} = \mathbf{h}_c(\mathbf{x}, \mathbf{u}) + \mathbf{v}_c \end{cases}, \quad (2)$$

where the state variable \mathbf{x} , input signal \mathbf{u} and output vector \mathbf{y} are respectively

$$\mathbf{x} = [\delta^T \ \omega^T \ e_q'^T \ e_d'^T]^T, \quad (3)$$

$$\mathbf{u} = [T_m^T \ E_{fd}^T]^T, \quad (4)$$

$$\mathbf{y} = \begin{bmatrix} e_{\mathbf{R}}^{\top} & e_{\mathbf{I}}^{\top} & i_{\mathbf{R}}^{\top} & i_{\mathbf{I}}^{\top} \end{bmatrix}^{\top}. \quad (5)$$

The i_{qi} , i_{di} , and T_{ei} in (1) are functions of \mathbf{x} :

$$\Psi_{\mathbf{R}i} = e'_{di} \sin \delta_i + e'_{qi} \cos \delta_i, \quad (6a)$$

$$\Psi_{\mathbf{I}i} = e'_{qi} \sin \delta_i - e'_{di} \cos \delta_i, \quad (6b)$$

$$I_{ti} = \bar{\mathbf{Y}}_i (\Psi_{\mathbf{R}} + j\Psi_{\mathbf{I}}), \quad (6c)$$

$$i_{\mathbf{R}i} = \text{Re}(I_{ti}), \quad (6d)$$

$$i_{\mathbf{I}i} = \text{Im}(I_{ti}), \quad (6e)$$

$$i_{qi} = \frac{S_{\mathbf{B}}}{S_{\mathbf{N}i}} (i_{\mathbf{I}i} \sin \delta_i + i_{\mathbf{R}i} \cos \delta_i), \quad (6f)$$

$$i_{di} = \frac{S_{\mathbf{B}}}{S_{\mathbf{N}i}} (i_{\mathbf{R}i} \sin \delta_i - i_{\mathbf{I}i} \cos \delta_i), \quad (6g)$$

$$e_{qi} = e'_{qi} - x'_{di} i_{di}, \quad (6h)$$

$$e_{di} = e'_{di} + x'_{qi} i_{qi}, \quad (6i)$$

$$P_{ei} = e_{qi} i_{qi} + e_{di} i_{di}, \quad (6j)$$

$$T_{ei} = \frac{S_{\mathbf{B}}}{S_{\mathbf{N}i}} P_{ei}. \quad (6k)$$

In (6), the output signals $i_{\mathbf{R}}$ and $i_{\mathbf{I}}$ are written as functions of \mathbf{x} ; and the outputs $e_{\mathbf{R}i}$ and $e_{\mathbf{I}i}$ can be expressed by

$$e_{\mathbf{R}i} = e_{di} \sin \delta_i + e_{qi} \cos \delta_i, \quad (7)$$

$$e_{\mathbf{I}i} = e_{qi} \sin \delta_i - e_{di} \cos \delta_i. \quad (8)$$

B. Discrete Model of Multi-Machine Power System With Partial Missing Measurements

Based on the continuous model expressed in (2), the discrete time state-space model of multi-machine power system with partial missing measurements can be derived as follows:

$$\begin{cases} \mathbf{x}_k = \mathbf{f}(\mathbf{x}_{k-1}, \mathbf{u}_{k-1}) + \mathbf{w}_k \\ \mathbf{y}_k = \mathbf{\Xi}_k \mathbf{h}(\mathbf{x}_k, \mathbf{u}_k) + \mathbf{v}_k \end{cases}, \quad (9)$$

where the subscript k denotes the time instant at $k\Delta t$, Δt indicates the sampling period; \mathbf{w}_k and \mathbf{v}_k are the system noise and measurement noise vector, which are usually consider as Gaussian white noise with zero mean. Let $\text{diag}\{\cdot\}$ represents the diagonal matrix, $\mathbf{\Xi}_k = \text{diag}\{\gamma_k^1, \gamma_k^2, \dots, \gamma_k^m\}$ and γ_k^i ($i = 1, 2, \dots, m$) represent the random variables in k and i , which are independent of the system noise and measurement noise. In addition $\mathbf{h}(\mathbf{x}_k, \mathbf{u}_k) = [\mathbf{h}^1(\mathbf{x}_k), \mathbf{h}^2(\mathbf{x}_k), \dots, \mathbf{h}^m(\mathbf{x}_k)]^{\top}$. It is assumed that the probability density function of γ_k^i on the interval $[0, 1]$ with the expectation $\bar{\mu}_k^i$ and the variance $\bar{\delta}_k^i$ ($i = 1, 2, \dots, m$). The system function is discretized by utilizing the modified Euler approach as follows [7]:

$$\tilde{\mathbf{x}}_k = \mathbf{x}_{k-1} + \mathbf{f}_c(\mathbf{x}_{k-1}, \mathbf{u}_{k-1}) \Delta t, \quad (10)$$

$$\tilde{\mathbf{f}} = \frac{\mathbf{f}_c(\tilde{\mathbf{x}}_k, \mathbf{u}_k) + \mathbf{f}_c(\mathbf{x}_{k-1}, \mathbf{u}_{k-1})}{2}, \quad (11)$$

$$\mathbf{x}_k = \mathbf{x}_{k-1} + \tilde{\mathbf{f}} \Delta t. \quad (12)$$

Remark 1: Unlike the previous research in [23]-[25], the partial measurement missing depicts the measurement fading phenomenon that maybe occur in reality [33]. It is used to

describe the attenuation degree of the measured signal. In this subsection, to characterize the partial measurement missing in the i th single measurement unit, the random variable γ_k^i with the value sampled from the uniform distribution of $[0, 1]$ interval is introduced. Therefore, the attenuation of the measurement information at a given time instant k can be determined by the random value of γ_k^i .

III. RESILIENT FAULT TOLERANT EKF APPROACH

In this part, a resilient fault tolerant EKF method for power system DSE with partial missing measurements is developed and the main procedures are presented in detail.

A. Basic Theory

For the sake of simplicity, some lemmas involved in the derivation will be introduced in advance.

Lemma 1: Given a matrix $\mathbf{A}_{m \times n}$ and a symmetric matrix $\mathbf{B}_{n \times n} = \mathbf{B}_{n \times n}^{\top}$, the partial derivative of $\text{tr}(\mathbf{A}\mathbf{B}\mathbf{A}^{\top})$ with respect to the matrix \mathbf{A} can be expressed by [33]:

$$\frac{\partial \text{tr}(\mathbf{A}\mathbf{B}\mathbf{A}^{\top})}{\partial \mathbf{A}} = 2\mathbf{A}\mathbf{B}, \quad (13)$$

where $\text{tr}(\cdot)$ represents the trace of the corresponding matrix.

Lemma 2: Given a real-valued matrix $\mathbf{A} = [a_{ij}]_{p \times p}$ and a diagonal random matrix $\mathbf{B} = \text{diag}(b_1, b_2, \dots, b_p)$, then the following equation can be derived [34]:

$$E(\mathbf{B}\mathbf{A}\mathbf{B}^{\top}) = \begin{bmatrix} E(b_1^2) E(b_1 b_2) \cdots E(b_1 b_p) \\ E(b_2 b_1) E(b_2^2) \cdots E(b_2 b_p) \\ \vdots \\ E(b_p b_1) E(b_p b_2) \cdots E(b_p^2) \end{bmatrix} \otimes \mathbf{A}, \quad (14)$$

where \otimes represents the Hadamard product, $E(\cdot)$ indicates the mathematical expectation.

For the sake of convenience, $\hat{\mathbf{x}}_k$ represents the estimator of \mathbf{x}_k , $\tilde{\mathbf{x}}_k$ denotes the prior estimator of \mathbf{x}_k , which are defined as follows:

$$\begin{cases} \hat{\mathbf{x}}_k = E[\mathbf{x}_k | \mathbf{y}_1, \mathbf{y}_2, \dots, \mathbf{y}_k] \\ \tilde{\mathbf{x}}_k = E[\mathbf{x}_k | \mathbf{y}_1, \mathbf{y}_2, \dots, \mathbf{y}_{k-1}] \end{cases}. \quad (15)$$

Considering the state-space model of power system in (10) with partial missing measurements, the following conditions needed to be satisfied

$$\begin{cases} E[\mathbf{w}_k] = 0, E[\mathbf{v}_k] = 0, E[\mathbf{w}_k \mathbf{v}_k^{\top}] = 0 \\ E[\mathbf{w}_k \mathbf{w}_j^{\top}] = \mathbf{Q}_k \Omega_{k-j}, E[\mathbf{v}_k \mathbf{v}_j^{\top}] = \mathbf{R}_k \Omega_{k-j} \\ \Omega_{k-j} = 1(k=j), \Omega_{k-j} = 0(k \neq j) \\ E[\mathbf{w}_k \mathbf{x}_0^{\top}] = 0, E[\mathbf{v}_k \mathbf{x}_0^{\top}] = 0 \end{cases}, \quad (16)$$

where Ω_{k-j} indicates the Kronecker delta function, $(\cdot)^{\top}$ represents the matrix transpose, $(\cdot)^{-1}$ denotes the inverse of a matrix. Then, the resilient fault tolerant EKF method for power system DSE with partial missing measurements can be developed.

B. Fault Tolerant EKF Method

To track the dynamics of multi-machine power system accurately with partial missing measurements, in this subsection,

we design a resilient dynamic state estimator of the following form:

$$\tilde{\mathbf{x}}_{k+1} = \mathbf{f}(\hat{\mathbf{x}}_k, \mathbf{u}_k), \quad (17)$$

$$\hat{\mathbf{x}}_{k+1} = \tilde{\mathbf{x}}_{k+1} + \mathbf{K}_{k+1} [\mathbf{y}_{k+1} - \bar{\boldsymbol{\Xi}}_{k+1} \mathbf{h}(\tilde{\mathbf{x}}_{k+1}, \mathbf{u}_{k+1})], \quad (18)$$

where $\tilde{\mathbf{x}}_{k+1}$, $\hat{\mathbf{x}}_{k+1}$ are respectively state prediction and state estimation at the time instant k ; \mathbf{K}_{k+1} indicates the gain of dynamic state estimator to be designed.

Denoting the state prediction error by $\tilde{\mathbf{e}}_{k+1} = \mathbf{x}_{k+1} - \tilde{\mathbf{x}}_{k+1}$ and the state estimation error by $\hat{\mathbf{e}}_{k+1} = \mathbf{x}_{k+1} - \hat{\mathbf{x}}_{k+1}$, we have

$$\tilde{\mathbf{P}}_{k+1} = E[\tilde{\mathbf{x}}_{k+1} \tilde{\mathbf{x}}_{k+1}^T], \quad (19)$$

$$\hat{\mathbf{P}}_{k+1} = E[\hat{\mathbf{x}}_{k+1} \hat{\mathbf{x}}_{k+1}^T]. \quad (20)$$

The purpose of this paper is to design a dynamic state estimator (19) and (20) such that: (i) an upper bound $\Psi_{k+1|k+1}$ is guaranteed for the state estimation error covariance matrix $\hat{\mathbf{P}}_{k+1}$; (ii) an appropriate gain of the state estimator \mathbf{K}_{k+1} is designed to minimize such an upper bound $\Psi_{k+1|k+1}$ at each time instant.

The detailed derivation of the proposed resilient dynamic state estimator is presented in the Appendix, it can be implemented by the following sequential steps:

1) Initialization

In this step, to initialize the FTEKF, the states and state covariance matrix are set up at $k = 0$, which can be expressed by

$$\hat{\mathbf{x}}_0 = E[\mathbf{x}_0], \quad (21)$$

$$\hat{\mathbf{P}}_0 = E[(\mathbf{x}_0 - \hat{\mathbf{x}}_0)(\mathbf{x}_0 - \hat{\mathbf{x}}_0)^T], \quad (22)$$

where $\hat{\mathbf{P}}_0$ denotes the posterior state estimation error covariance.

2) State Prediction

For each time instant k , the prediction of state and corresponding covariance matrix can be done as follows.

a) Partial derivative matrix of the current state estimate $\hat{\mathbf{x}}_{k-1}$ is calculated by

$$\mathbf{F}_{k-1} = \left. \frac{\partial \mathbf{f}(\mathbf{x}_{k-1}, \mathbf{u}_{k-1})}{\partial \mathbf{x}_{k-1}} \right|_{\mathbf{x}_{k-1} = \hat{\mathbf{x}}_{k-1}}. \quad (23)$$

b) The time update of state prediction $\tilde{\mathbf{x}}_k$ and estimation error covariance matrix $\tilde{\mathbf{P}}_k$ at time instant k is performed by utilizing

$$\tilde{\mathbf{x}}_k = \mathbf{f}(\hat{\mathbf{x}}_{k-1}, \mathbf{u}_{k-1}), \quad (24)$$

$$\tilde{\mathbf{P}}_k = \mathbf{F}_{k-1} \hat{\mathbf{P}}_{k-1} \mathbf{F}_{k-1}^T + \mathbf{Q}_k, \quad (25)$$

where $\hat{\mathbf{x}}_{k-1}$ and $\hat{\mathbf{P}}_{k-1}$ are the estimated state and state estimation error covariance matrix at time instant $k - 1$, respectively.

3) State Update

For each time instant k , the posterior state vector and the predicted error covariance matrix can be updated as follows.

a) Partial derivative matrix for the correction is calculated by

$$\mathbf{H}_k = \left. \frac{\partial \mathbf{h}(\mathbf{x}_k)}{\partial \mathbf{x}_k} \right|_{\mathbf{x}_k = \tilde{\mathbf{x}}_k}. \quad (26)$$

b) Calculate the Kalman filter gain at time instant k

$$\mathbf{K}_k = \left(\tilde{\mathbf{P}}_k \mathbf{H}_k^T \bar{\boldsymbol{\Xi}}_k^T \right) \times \left[\bar{\boldsymbol{\Xi}}_k \mathbf{H}_k \tilde{\mathbf{P}}_k \mathbf{H}_k^T \bar{\boldsymbol{\Xi}}_k^T + E \left(\tilde{\boldsymbol{\Xi}}_k \mathbf{h}(\tilde{\mathbf{x}}_k) \mathbf{h}^T(\tilde{\mathbf{x}}_k) \tilde{\boldsymbol{\Xi}}_k^T \right) + \mathbf{R}_k \right]^{-1}, \quad (27)$$

where $\bar{\boldsymbol{\Xi}}_k = E(\boldsymbol{\Xi}_k) = \text{diag}(\bar{\mu}_k^1, \bar{\mu}_k^2, \dots, \bar{\mu}_k^m)$ and $\tilde{\boldsymbol{\Xi}}_{k+1} = \boldsymbol{\Xi}_{k+1} - \bar{\boldsymbol{\Xi}}_{k+1}$.

c) The measurement update of the estimated state $\hat{\mathbf{x}}_k$ at the time instant k is performed by

$$\hat{\mathbf{x}}_k = \tilde{\mathbf{x}}_k + \mathbf{K}_k [\mathbf{y}_k - \bar{\boldsymbol{\Xi}}_k \mathbf{h}(\tilde{\mathbf{x}}_k)]. \quad (28)$$

d) The measurement update of the estimation error covariance $\hat{\mathbf{P}}_k$ at the time instant k is calculated by

$$\begin{aligned} \hat{\mathbf{P}}_k &= (\mathbf{I} - \mathbf{K}_k \bar{\boldsymbol{\Xi}}_k \mathbf{H}_k) \tilde{\mathbf{P}}_k \\ &\quad \times (\mathbf{I} - \mathbf{K}_k \bar{\boldsymbol{\Xi}}_k \mathbf{H}_k)^T + \mathbf{K}_k \mathbf{R}_k \mathbf{K}_k^T \\ &\quad + \mathbf{K}_k E \left[\tilde{\boldsymbol{\Xi}}_k \mathbf{h}(\tilde{\mathbf{x}}_k) \mathbf{h}^T(\tilde{\mathbf{x}}_k) \tilde{\boldsymbol{\Xi}}_k^T \right] \mathbf{K}_k^T \end{aligned} \quad (29)$$

Finally, for the sake of simplicity, the proposed resilient fault tolerant EKF method is summarized as Algorithm 1.

Algorithm 1: Fault Tolerant EKF Method

- 1: Initialization: set the initial values for $\hat{\mathbf{x}}_0$, $\hat{\mathbf{P}}_0$, T_s ;
 - 2: Input: partial missing measurements \mathbf{y}_k ;
 - 3: **while** $k = 0$ to T_s **do**
 - 4: **Step 1:** compute the value of predicted state
 - 5: $\tilde{\mathbf{x}}_k \leftarrow \mathbf{f}(\hat{\mathbf{x}}_{k-1}, \mathbf{u}_{k-1})$;
 - 6: **Step 2:** calculate the covariance matrix of state prediction error
 - 7: $\tilde{\mathbf{P}}_k \leftarrow \mathbf{F}_{k-1} \hat{\mathbf{P}}_{k-1} \mathbf{F}_{k-1}^T + \mathbf{Q}_k$;
 - 8: **Step 3:** calculate the Kalman filter gain matrix
 - 9: $\mathbf{K}_k \leftarrow \left(\tilde{\mathbf{P}}_k \mathbf{H}_k^T \bar{\boldsymbol{\Xi}}_k^T \right) \times \left[\bar{\boldsymbol{\Xi}}_k \mathbf{H}_k \tilde{\mathbf{P}}_k \mathbf{H}_k^T \bar{\boldsymbol{\Xi}}_k^T + E \left(\tilde{\boldsymbol{\Xi}}_k \mathbf{h}(\tilde{\mathbf{x}}_k) \mathbf{h}^T(\tilde{\mathbf{x}}_k) \tilde{\boldsymbol{\Xi}}_k^T \right) + \mathbf{R}_k \right]^{-1}$;
 - 10: **Step 4:** update the predicted state vector with measurement \mathbf{y}_k
 - 11: $\hat{\mathbf{x}}_k \leftarrow \tilde{\mathbf{x}}_k + \mathbf{K}_k [\mathbf{y}_k - \bar{\boldsymbol{\Xi}}_k \mathbf{h}(\tilde{\mathbf{x}}_k)]$;
 - 12: **Step 5:** update the covariance matrix of state estimation error
 - 13: $\hat{\mathbf{P}}_k = (\mathbf{I} - \mathbf{K}_k \bar{\boldsymbol{\Xi}}_k \mathbf{H}_k) \tilde{\mathbf{P}}_k$
 $\times (\mathbf{I} - \mathbf{K}_k \bar{\boldsymbol{\Xi}}_k \mathbf{H}_k)^T + \mathbf{K}_k \mathbf{R}_k \mathbf{K}_k^T$
 $+ \mathbf{K}_k E \left[\tilde{\boldsymbol{\Xi}}_k \mathbf{h}(\tilde{\mathbf{x}}_k) \mathbf{h}^T(\tilde{\mathbf{x}}_k) \tilde{\boldsymbol{\Xi}}_k^T \right] \mathbf{K}_k^T$;
 - 14: **Step 6:** output the state variable $\hat{\mathbf{x}}_k$, the estimation error covariance $\hat{\mathbf{P}}_k$, and update the time instant
 - 15: $k \leftarrow k + 1$;
 - 16: **end while**
-

Remark 2: In the design of fault tolerant EKF method, it is not necessary to know precisely the occurrence time instant of sensor data loss, this reflects the actual conditions of power system and guarantees its good applicability. Nonetheless, the statistical law of the partial missing measurements is needed, which can be acquired through statistical tests.

IV. SIMULATION RESULTS AND ANALYSIS

To validate the resilience of fault tolerant EKF approach against partial missing measurements, extensive simulations are implemented on the WECC system, the New England system and the NPCC system. In addition, the classic EKF and UKF approaches come from EKF/UKF Toolbox [35] are also carried out for comparisons.

A. Test Systems

The specific parameters and fault conditions of each test system are set as follows.

- 1) **WECC 9-bus System**: This test system includes three synchronous generators and three load points with the total loading of 115MVar and 315MW, whose data and configuration can be found in [32]. At $t=1s$, a fault is occurred near the bus 8 and the line 8-9 is cleared after 2 cycles, which results in a disturbance to the WECC test system.
- 2) **New England 39-bus System**: This system contains ten synchronous generators, 21 load points with the total loading of 1378.1MVar and 6254.2MW. The detailed parameters and topology information of this test system can be seen in [36]. In the simulations, a fault is applied to the place near bus 4 of the system after 1 second, which is cleared after 2 cycles by removing the line between the bus 4 and bus 14.
- 3) **NPCC 140-bus System**: The NPCC system indicates the northeast region of the EI system. This system includes forty eight synchronous generators and 140 buses. The detailed parameters and topology information of this test system can be found in [13], [38].

In order to effectively reduce the integral error and precisely capture the dynamic features of each discussed test system, where the simulation time step is set as 0.001 second. Then, to accurately mimic the field measurements measured by PMUs, the simulated data is sampled to 50 samples per second with the additional noise is added. It's worth pointing out that all the discussed approaches are performed in MATLAB R2016b on a PC with the Intel Core CPU E5-1650, 3.5 GHz and 32 GB RAM.

Furthermore, in order to acquire a more general and significant result, $N_{MC}=200$ Monte-Carlo simulations are running for all the case studies. The performance metric based on the \mathcal{L}_1 norm is utilized to quantitatively compare the estimation results, which is defined as follows:

$$e_x = \frac{1}{N_{MC}} \sum_{j=1}^{N_{MC}} \frac{1}{T_s} \sum_{k=1}^{T_s} \left[\frac{1}{n} \sum_{i=1}^n |x_{i,k}^{est} - x_{i,k}^{true}| \right], \quad (30)$$

where k represents the time instant; T_s indicates the total simulation time steps, n represents the number of generators in the test system; x denotes a type of generator states that can be δ , ω , e'_q , or e'_d ; $x_{i,k}^{est}$ represents the estimated state and $x_{i,k}^{true}$ indicates the corresponding true value of generator i at time instant k .

B. WECC 9-bus System

In this case, the conventional EKF, UKF and the proposed

FTEKF method are tested on the WECC system. To make the mathematics easy to understand, the second-order classical model are utilized for all the generators in this test system. In the simulation studies, the standard deviation of system and measurement noise is set as 10^{-2} ; the initial values of the estimation error covariance matrix for the EKF, UKF and the proposed FTEKF approaches are set as $10^{-4} I_{2n \times 2n}$. The initial states are obtained by the steady-state power flow calculation.

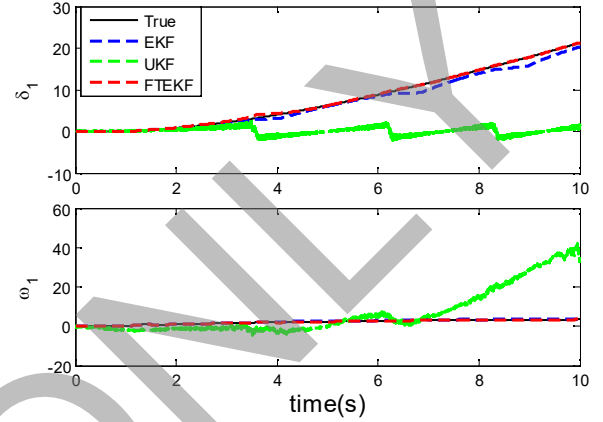


Fig. 1. Estimation results of δ_1, ω_1 for generator 1 of WECC 9-bus system with partial missing measurements.

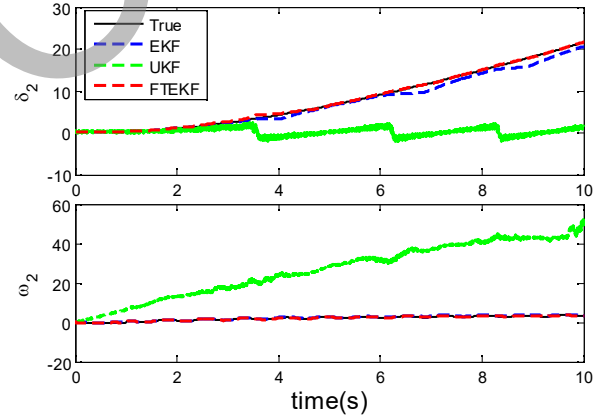


Fig. 2. Estimation results of δ_2, ω_2 for generator 2 of WECC 9-bus system with partial missing measurements.

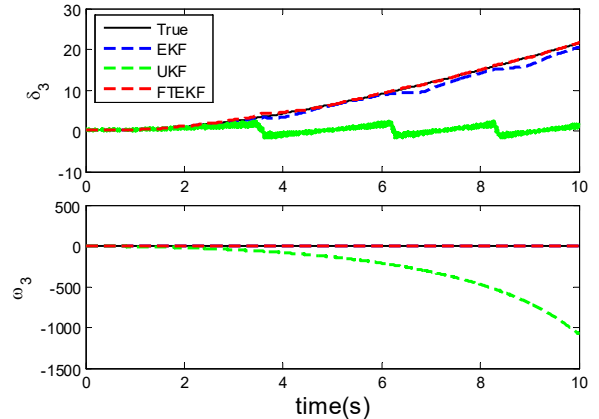


Fig. 3. Estimation results of δ_3, ω_3 for generator 3 of WECC 9-bus system with partial missing measurements.

Figs. 1-3 show the estimation performance of EKF, UKF,

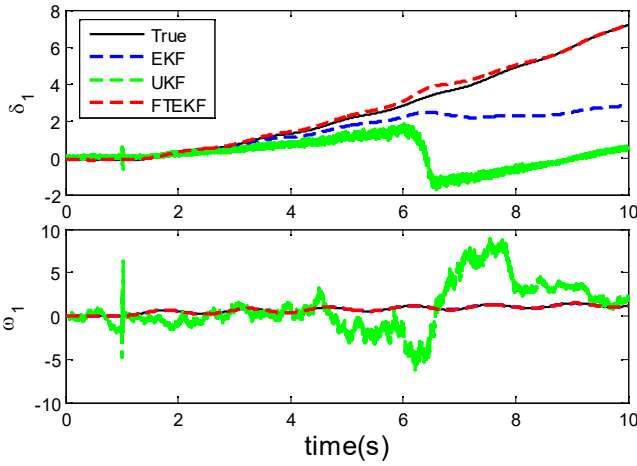


Fig. 4. Estimation results of δ_1, ω_1 for generator 1 of New England 39-bus system with partial missing measurements.

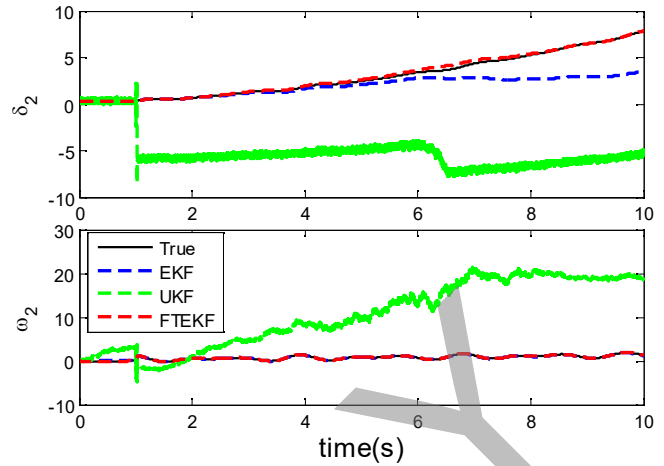


Fig. 5. Estimation results of δ_2, ω_2 for generator 2 of New England 39-bus system with partial missing measurements.

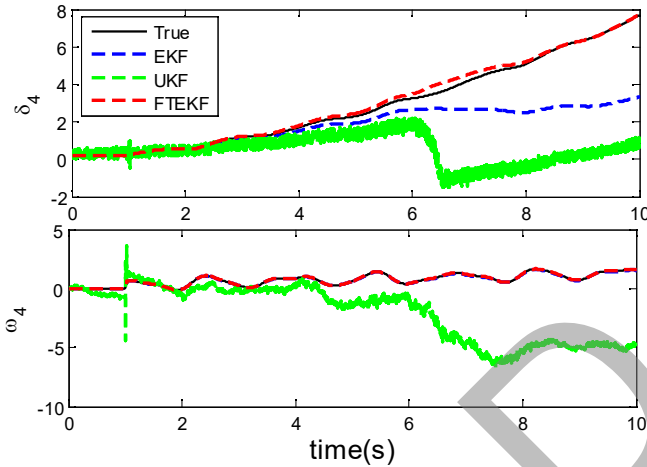


Fig. 6. Estimation results of δ_4, ω_4 for generator 4 of New England 39-bus system with partial missing measurements.

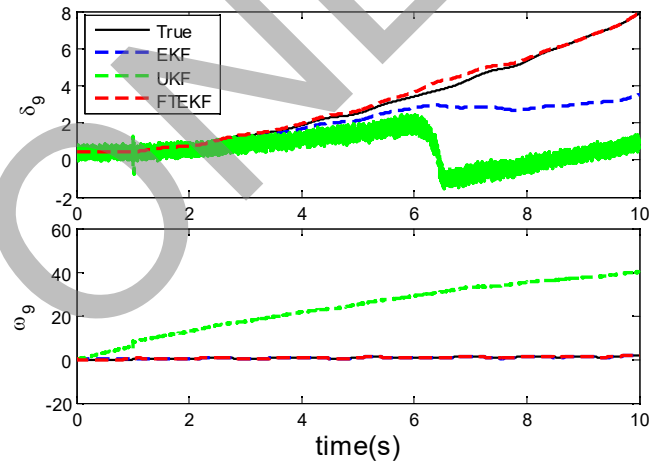


Fig. 7. Estimation results of δ_9, ω_9 for generator 9 of New England 39-bus system with partial missing measurements.

TABLE I
PERFORMANCE COMPARISON OF EKF, UKF AND FTEKF FOR WECC-9 BUS SYSTEM WITH PARTIAL MISSING MEASUREMENTS

Metric	EKF	UKF	FTEKF
e_δ	0.5901	7.7831	0.1259
e_ω	0.2501	95.2186	0.0378

TABLE II
PERFORMANCE COMPARISON OF EKF, UKF AND FTEKF FOR NEW ENGLAND-39 BUS SYSTEM WITH PARTIAL MISSING MEASUREMENTS

Metric	EKF	UKF	FTEKF
e_δ	1.1903	3.0148	0.1206
e_ω	0.0327	10.5028	0.0101

and the proposed FTEKF. As is shown in the figures, the proposed fault tolerant EKF can track the dynamic states of each synchronous generator in the WECC system accurately even by utilizing the partial missing measurements, and provides the better performance than the other discussed approaches.

To be specific, the standard EKF and UKF methods are failing to provide the reliable estimate results, which reflects that they are sensitive to the sensor data loss. Furthermore, it can be noticed that unlike EKF and FTEKF approaches, the UKF method exhibits numerical instabilities in the presence of partial missing measurements.

In addition, the performance indices of the conventional EKF, UKF and the proposed FTEKF approaches for the WECC test system DSE with partial missing measurements are summarized in Table 1. It can be found that the estimation error of the proposed FTEKF is much smaller than the other methods. These experimental results are in agreement with the earlier observations, which further confirm the developed FTEKF method is more robust and resilient against the sensor data loss.

C. New England 39-bus System

In this scenario, all the discussed approaches are implemented on the New England test system. All generators in this test system are also assumed to have second-order classical model. The standard deviation of system and measurement noise is still set as 10^{-2} ; the error covariance matrix of state

TABLE III
PERFORMANCE COMPARISON OF EKF, UKF AND FTEKF FOR NPCC-140 BUS SYSTEM WITH PARTIAL MISSING MEASUREMENTS.

Metric	EKF	UKF	FTEKF
e_{δ}	1.6107	56.5049	0.1194
e_{ω}	2.2584	30.9248	0.1597
$e_{e'_q}$	5.0257	10.3269	0.0326
$e_{e'_d}$	16.1305	7.5742	0.0184

estimation for each discussed methods is the same, which is initialized as $10^{-4}\mathbf{I}_{2n \times 2n}$.

The tracking results of EKF, UKF and the proposed method are shown in Figs. 4-7. Due to the page limit, only the generator 1, 2, 4 and 9 are randomly picked as examples, and the remaining plots are omitted due to they do not contain any additional valid information. It can be observed that the UKF method cannot track the states of test system precisely, which encounters numerical stability problem and makes its state estimation result diverge. The EKF approach can obtain a better estimation performance than the standard UKF method, but its estimation accuracy is still not acceptable. By contrast, the FTEKF exhibits strong robustness and resilient against partial missing measurements, resulting in the best state estimation performance.

Similar to the WECC test system scenario, the estimation error indices of each discussed approaches are also calculated and summarized in the Table II. It can be seen that FTEKF owns the smallest estimation error indices. These experimental results are consistent with data obtained in the WECC system.

D. NPCC 140-bus System

The classical second-order model of generator is simple and clear, and the interface between the generator and the power grid is convenient. However, it cannot be utilized to track the transient voltages e'_q and e'_d . Therefore, to further demonstrate the efficacy of the proposed fault tolerant EKF and confirm its scalability, the discussed methods are performed on the NPCC test system [38]. Twenty seven generators utilize fourth-order model and the remainder 21 have second-order classical model. In this scenario, the standard deviation of system and measurement noise is set as 10^{-2} ; the initial values of the estimation error covariance matrix for the EKF, UKF and the proposed FTEKF approaches are set as $10^{-4}\mathbf{I}_{150 \times 150}$.

We implemented dynamic state estimation for each of the discussed approaches and calculated the average values of the system state estimation error index. The estimation results of EKF, UKF and the developed FTEKF method are presented in Figs. 8 and 9, due to space limitation, only the generator 6 is randomly picked as an example. The estimation error index of each discussed methods are also presented in Table III.

As is shown in the figures, the estimated states from the conventional EKF and UKF quickly diverge from the true values; this reflects that they are sensitive to the partial missing measurements. In contrast, the proposed FTEKF method is still able to track the states of test system accurately. These

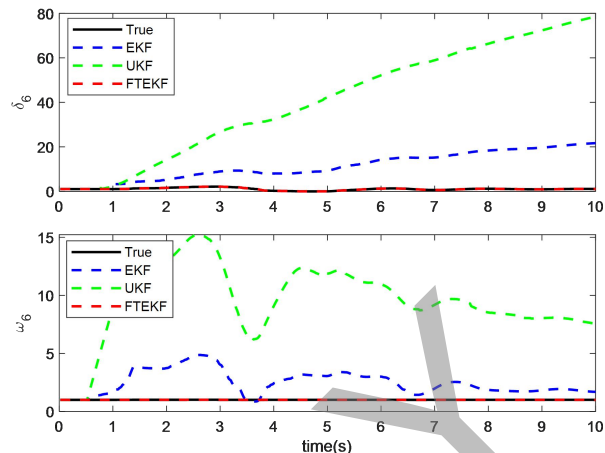


Fig. 8. Estimation results of δ_6, ω_6 for generator 6 of NPCC 140-bus system with partial missing measurements.

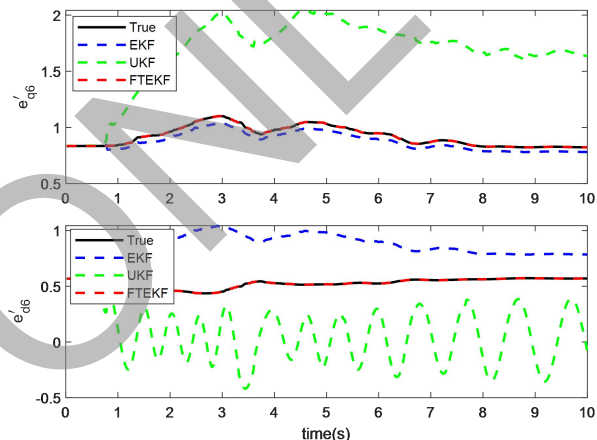


Fig. 9. Estimation results of e'_{q6}, e'_{d6} for generator 6 of NPCC 140-bus system with partial missing measurements.

estimation results are not only further confirm the strong robustness of the FTEKF against partial missing measurements but also demonstrate its good scalability.

E. Centralized versus Decentralized FTEKF

To meet the various advanced real-time applications of EMS, the DSE approach for power system must have a good computational efficiency. Therefore, to inspect whether the developed FTEKF is able to catch up with PMUs at the sampled rate between 30 samples/s and 60 samples/s. Fig. 10 shows the total running time of each of the discussed approaches for the different test systems, which is the average time of 200 Monte Carlo experiments under various conditions. These experimental data verify that EKF, UKF and the proposed FTEKF almost have the similar computing efficiency for the same test system. To be specific, the execution time of FTEKF is slightly larger than that of EKF, due to the more complicated formulas. In addition, due to the utilization of high-order generator model and the increase of system scale, the calculation time of different methods for the NPCC system increases significantly. However, the execution time of all the discussed methods is much less than the sampling period 16.7 ms (60 samples/s).

Furthermore, it's worth noting that although the proposed

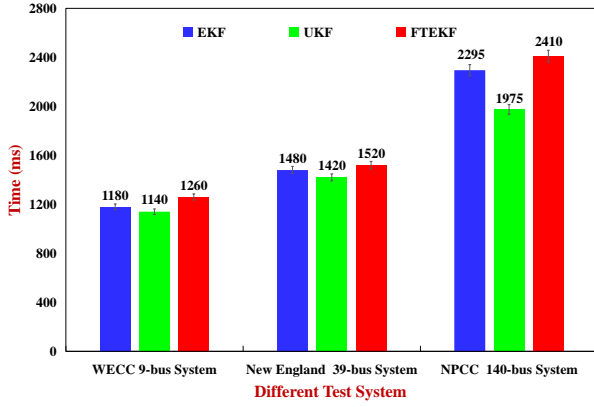


Fig. 10. Total execution time of each discussed approach for different test system.

FTEKF method is implemented in a centralized way, it can also be executed in a distributed form. The results show that FTEKF approach has good scalability and can be applied to multi-machine power system. For instance, by adopting the method in [37], the dynamic equations of each generation unit can be decoupled from system. Then, the resilient FTEKF can be adopted to track the dynamic state variable of system with only local PMU measurements. Therefore, the computational efficiency of FTEKF can satisfy the needs of large scale multi-machine power system calculation and analysis.

V. CONCLUSIONS

Accurate dynamic state estimation under measurement noise and partial missing measurements is critical for the energy management system in modern smart grid. To deal with these issues, in this paper, a discrete distribution in the interval [0,1] was introduced to model and depict the partial missing measurements of power system first. Subsequently, a robust and resilient fault tolerant EKF approach has been designed to mitigate the adverse influence of partial missing measurements on the state estimation accuracy. Experimental data demonstrate that the proposed method can acquire superior estimation accuracy than the standard EKF and UKF methods for different test system with partial missing measurements, which has the strong robustness and resilience against sensor failure. However, it is worth pointing out that the inputs in the model are assumed to be known, which sometimes may not be the case in reality. The dynamic state estimation of power system with unknown inputs (T_m or E_{fd}) under the framework of this paper will be specially investigated in the future.

APPENDIX

In this section, the detailed derivation process of the proposed FTEKF approach are presented.

Proof:

Considering the state space model in (10), if the conditions in (21) are satisfied, the proposed recursive filter can be formulated as follows

$$\tilde{\mathbf{x}}_{k+1} = \mathbf{f}(\hat{\mathbf{x}}_k, \mathbf{u}_k), \quad (31)$$

$$\hat{\mathbf{x}}_{k+1} = \tilde{\mathbf{x}}_{k+1} + \mathbf{K}_{k+1} [\mathbf{y}_{k+1} - \bar{\boldsymbol{\Xi}}_{k+1} \mathbf{h}(\tilde{\mathbf{x}}_{k+1}, \mathbf{u}_{k+1})]. \quad (32)$$

Based on (9), (31) and (32), the prior state estimation error $\tilde{\mathbf{e}}_{k+1}$ and the posterior state estimation error $\hat{\mathbf{e}}_{k+1}$ can be calculated by

$$\begin{aligned} \tilde{\mathbf{e}}_{k+1} &= \mathbf{x}_{k+1} - \tilde{\mathbf{x}}_{k+1} \\ &= \mathbf{f}(\mathbf{x}_k, \mathbf{u}_k) + \mathbf{w}_k - \mathbf{f}(\hat{\mathbf{x}}_k, \mathbf{u}_k), \end{aligned} \quad (33)$$

$$\begin{aligned} \hat{\mathbf{e}}_{k+1} &= \mathbf{x}_{k+1} - \hat{\mathbf{x}}_{k+1} = \mathbf{f}(\mathbf{x}_k, \mathbf{u}_k) + \mathbf{w}_k - \tilde{\mathbf{x}}_{k+1} \\ &\quad - \mathbf{K}_{k+1} [\mathbf{y}_{k+1} - \bar{\boldsymbol{\Xi}}_{k+1} \mathbf{h}(\tilde{\mathbf{x}}_{k+1}, \mathbf{u}_{k+1})]. \end{aligned} \quad (34)$$

Expanding $\mathbf{f}(\cdot)$ and $\mathbf{h}(\cdot)$ into Taylor series at $\hat{\mathbf{x}}_k$ and $\tilde{\mathbf{x}}_{k+1}$, respectively. After neglecting the higher order terms, the following equations can be derived

$$\begin{cases} \mathbf{f}(\mathbf{x}_k, \mathbf{u}_k) = \mathbf{f}(\hat{\mathbf{x}}_k, \mathbf{u}_k) + \mathbf{F}_k \hat{\mathbf{e}}_k \\ \mathbf{F}_k = \left. \frac{\partial \mathbf{f}(\mathbf{x}_k, \mathbf{u}_k)}{\partial \mathbf{x}_k} \right|_{\mathbf{x}_k = \hat{\mathbf{x}}_k} \end{cases}, \quad (35)$$

$$\begin{cases} \mathbf{h}(\mathbf{x}_{k+1}, \mathbf{u}_{k+1}) = \mathbf{h}(\tilde{\mathbf{x}}_{k+1}, \mathbf{u}_{k+1}) + \mathbf{H}_{k+1} \tilde{\mathbf{e}}_{k+1} \\ \mathbf{H}_{k+1} = \left. \frac{\partial \mathbf{h}(\mathbf{x}_{k+1}, \mathbf{u}_{k+1})}{\partial \mathbf{x}_{k+1}} \right|_{\mathbf{x}_{k+1} = \tilde{\mathbf{x}}_{k+1}} \end{cases}. \quad (36)$$

Utilizing (35)-(36), the equations (33) and (34) can be approximated by

$$\tilde{\mathbf{e}}_{k+1} = \mathbf{F}_k \hat{\mathbf{e}}_k + \mathbf{w}_k, \quad (37)$$

$$\begin{aligned} \hat{\mathbf{e}}_{k+1} &= \mathbf{f}(\hat{\mathbf{x}}_k, \mathbf{u}_k) + \mathbf{F}_k \hat{\mathbf{e}}_k + \mathbf{w}_k - \mathbf{f}(\hat{\mathbf{x}}_k, \mathbf{u}_k) \\ &\quad - \mathbf{K}_{k+1} \left[\begin{array}{c} (\bar{\boldsymbol{\Xi}}_{k+1} - \bar{\boldsymbol{\Xi}}_{k+1}) \mathbf{h}(\tilde{\mathbf{x}}_{k+1}, \mathbf{u}_{k+1}) \\ + \mathbf{v}_{k+1} + \bar{\boldsymbol{\Xi}}_{k+1} \mathbf{H}_{k+1} \tilde{\mathbf{e}}_{k+1} \end{array} \right] \\ &= (\mathbf{I} - \mathbf{K}_{k+1} \bar{\boldsymbol{\Xi}}_{k+1} \mathbf{H}_{k+1}) \tilde{\mathbf{e}}_{k+1} \\ &\quad - \mathbf{K}_{k+1} \bar{\boldsymbol{\Xi}}_{k+1} \mathbf{h}(\tilde{\mathbf{x}}_{k+1}, \mathbf{u}_{k+1}) - \mathbf{K}_{k+1} \mathbf{v}_{k+1}. \end{aligned} \quad (38)$$

According to (37), the error covariance matrix of state prediction $\tilde{\mathbf{P}}_{k+1}$ at the time instant $k+1$ can be derived as follows

$$\begin{aligned} \tilde{\mathbf{P}}_{k+1} &= E \left[\tilde{\mathbf{e}}_{k+1} (\tilde{\mathbf{e}}_{k+1})^T \right] \\ &= \mathbf{F}_k \hat{\mathbf{P}}_k \mathbf{F}_k^T + \mathbf{Q}_k. \end{aligned} \quad (39)$$

Similarly, the posterior state estimation error covariance matrix $\hat{\mathbf{P}}_{k+1}$ can be evolved as

$$\begin{aligned} \hat{\mathbf{P}}_{k+1} &= E \left[\hat{\mathbf{e}}_{k+1} (\hat{\mathbf{e}}_{k+1})^T \right] \\ &= E \left\{ \left[(\mathbf{I} - \mathbf{K}_{k+1} \bar{\boldsymbol{\Xi}}_{k+1} \mathbf{H}_{k+1}) \tilde{\mathbf{e}}_{k+1} - \mathbf{K}_{k+1} \mathbf{v}_{k+1} \right. \right. \\ &\quad \left. \left. - \mathbf{K}_{k+1} \bar{\boldsymbol{\Xi}}_{k+1} \mathbf{h}(\tilde{\mathbf{x}}_{k+1}, \mathbf{u}_{k+1}) \right] \right. \\ &\quad \times \left. \left[(\mathbf{I} - \mathbf{K}_{k+1} \bar{\boldsymbol{\Xi}}_{k+1} \mathbf{H}_{k+1}) \tilde{\mathbf{e}}_{k+1} - \mathbf{K}_{k+1} \mathbf{v}_{k+1} \right. \right. \\ &\quad \left. \left. - \mathbf{K}_{k+1} \bar{\boldsymbol{\Xi}}_{k+1} \mathbf{h}(\tilde{\mathbf{x}}_{k+1}, \mathbf{u}_{k+1}) \right]^T \right\} \\ &= \sum_{\hat{m}=1}^3 \sum_{\hat{n}=1}^3 \hat{\mathbf{P}}_{k+1}(\hat{m}\hat{n}), \end{aligned} \quad (40)$$

where $\hat{P}_{k+1}(\hat{m}\hat{n})$ are equal to the following:

$$\hat{P}_{k+1}(11) = (\mathbf{I} - \mathbf{K}_{k+1}\mathbf{\Xi}_{k+1}\mathbf{H}_{k+1})\tilde{P}_{k+1} \times (\mathbf{I} - \mathbf{K}_{k+1}\mathbf{\Xi}_{k+1}\mathbf{H}_{k+1})^T, \quad (41)$$

$$\hat{P}_{k+1}(22) = \mathbf{K}_{k+1}E(\mathbf{v}_{k+1}\mathbf{v}_{k+1}^T)\mathbf{K}_{k+1}^T = \mathbf{K}_{k+1}\mathbf{R}_{k+1}\mathbf{K}_{k+1}^T, \quad (42)$$

$$\hat{P}_{k+1}(33) = \mathbf{K}_{k+1}E \begin{bmatrix} \tilde{\mathbf{\Xi}}_{k+1}\mathbf{h}(\tilde{\mathbf{x}}_{k+1}, \mathbf{u}_{k+1}) \times \\ \mathbf{h}^T(\tilde{\mathbf{x}}_{k+1}, \mathbf{u}_{k+1})\tilde{\mathbf{\Xi}}_{k+1}^T \end{bmatrix} \times \mathbf{K}_{k+1}^T, \quad (43)$$

$$\hat{P}_{k+1}(12) = -(\mathbf{I} - \mathbf{K}_{k+1}\mathbf{\Xi}_{k+1}\mathbf{H}_{k+1}) \times E(\tilde{\mathbf{e}}_{k+1}\mathbf{v}_{k+1})^T\mathbf{K}_{k+1}^T, \quad (44)$$

$$\hat{P}_{k+1}(13) = -(\mathbf{I} - \mathbf{K}_{k+1}\mathbf{\Xi}_{k+1}\mathbf{H}_{k+1}) \times E \left[\tilde{\mathbf{e}}_{k+1}\mathbf{h}^T(\tilde{\mathbf{x}}_{k+1}, \mathbf{u}_{k+1})\tilde{\mathbf{\Xi}}_{k+1}^T \right] \mathbf{K}_{k+1}^T, \quad (45)$$

$$\hat{P}_{k+1}(23) = \mathbf{K}_{k+1}E(\mathbf{v}_{k+1}\mathbf{h}^T(\tilde{\mathbf{x}}_{k+1}, \mathbf{u}_{k+1})\tilde{\mathbf{\Xi}}_{k+1}^T)\mathbf{K}_{k+1}^T, \quad (46)$$

$$\hat{P}_{k+1}(21) = \left(\hat{P}_{k+1}(12) \right)^T, \quad (47)$$

$$\hat{P}_{k+1}(31) = \left(\hat{P}_{k+1}(13) \right)^T, \quad (48)$$

$$\hat{P}_{k+1}(32) = \left(\hat{P}_{k+1}(23) \right)^T. \quad (49)$$

Due to \mathbf{w}_k , \mathbf{e}_k , \mathbf{v}_k and $\tilde{\mathbf{\Xi}}_{k+1}$ are mutually uncorrelated [23], [24], the results of $\hat{P}_{k+1}(12)$, $\hat{P}_{k+1}(13)$, $\hat{P}_{k+1}(23)$, $\hat{P}_{k+1}(21)$, $\hat{P}_{k+1}(31)$, $\hat{P}_{k+1}(32)$ are zeros. Therefore, (40) can be derived as follows

$$\hat{P}_{k+1} = (\mathbf{I} - \mathbf{K}_{k+1}\mathbf{\Xi}_{k+1}\mathbf{H}_{k+1})\tilde{P}_{k+1} \times (\mathbf{I} - \mathbf{K}_{k+1}\mathbf{\Xi}_{k+1}\mathbf{H}_{k+1})^T + \mathbf{K}_{k+1}\mathbf{R}_{k+1}\mathbf{K}_{k+1}^T + \mathbf{K}_{k+1}E \left[\tilde{\mathbf{\Xi}}_{k+1}\mathbf{h}(\tilde{\mathbf{x}}_{k+1}, \mathbf{u}_{k+1}) \times \mathbf{h}^T(\tilde{\mathbf{x}}_{k+1}, \mathbf{u}_{k+1})\tilde{\mathbf{\Xi}}_{k+1}^T \right] \mathbf{K}_{k+1}^T. \quad (50)$$

According to the Lemma 1, the following equation can be derived

$$\frac{\partial \text{tr}(\hat{P}_{k+1})}{\partial \mathbf{K}_{k+1}} = -2(\mathbf{I} - \mathbf{K}_{k+1}\mathbf{\Xi}_{k+1}\mathbf{H}_{k+1})\tilde{P}_{k+1}\mathbf{H}_{k+1}^T\mathbf{\Xi}_{k+1}^T + 2\mathbf{K}_{k+1} \left\{ E \left[\tilde{\mathbf{\Xi}}_{k+1}\mathbf{h}(\tilde{\mathbf{x}}_{k+1}, \mathbf{u}_{k+1}) \times \mathbf{h}^T(\tilde{\mathbf{x}}_{k+1}, \mathbf{u}_{k+1})\tilde{\mathbf{\Xi}}_{k+1}^T \right] \right\} + 2\mathbf{K}_{k+1}\mathbf{R}_{k+1}. \quad (51)$$

Let (51) equal to zero, the optimal filter gain \mathbf{K}_{k+1} can be acquired as follows

$$\mathbf{K}_{k+1} = \left(\tilde{P}_{k+1}\mathbf{H}_{k+1}^T\mathbf{\Xi}_{k+1}^T \right) \times \left[\mathbf{\Xi}_{k+1}\mathbf{H}_{k+1}\tilde{P}_{k+1}\mathbf{H}_{k+1}^T\mathbf{\Xi}_{k+1}^T + E \left(\tilde{\mathbf{\Xi}}_{k+1}\mathbf{h}(\tilde{\mathbf{x}}_{k+1}, \mathbf{u}_{k+1}) \times \mathbf{h}^T(\tilde{\mathbf{x}}_{k+1}, \mathbf{u}_{k+1})\tilde{\mathbf{\Xi}}_{k+1}^T \right) + \mathbf{R}_{k+1} \right]^{-1}. \quad (52)$$

Based on the Lemma 2, (52) can be reformulated as follows

$$\mathbf{K}_{k+1} = \left(\tilde{P}_{k+1}\mathbf{H}_{k+1}^T\mathbf{\Xi}_{k+1}^T \right) \times \left[\mathbf{\Xi}_{k+1}\mathbf{H}_{k+1}\tilde{P}_{k+1}\mathbf{H}_{k+1}^T\mathbf{\Xi}_{k+1}^T + \tilde{\mathbf{\Xi}}_{k+1} \otimes E(\mathbf{h}(\tilde{\mathbf{x}}_{k+1}, \mathbf{u}_{k+1})) \times \mathbf{h}^T(\tilde{\mathbf{x}}_{k+1}, \mathbf{u}_{k+1}) + \mathbf{R}_{k+1} \right]^{-1}. \quad (53)$$

This completes the proof of the developed FTEKF.

REFERENCES

- [1] D. Hou, Y. Sun, L. Zhang, and S. Wang, "Robust forecasting-aided state estimation considering uncertainty in distribution system," *CSEE Journal of Power and Energy Systems*, DOI: 10.17775/CSEEJPES.2020.07030, 2022.
- [2] Y. Wang, Y. Sun, and V. Dinavahi, "Robust forecasting-aided state estimation for power system against uncertainties," *IEEE Trans. Power Syst.*, vol. 35, no. 1, pp. 691-702, Jan. 2020.
- [3] H. Karimipour and V. Dinavahi, "Extended Kalman filter-based parallel dynamic state estimation," *IEEE Trans. Smart Grid*, vol. 6, no. 4, pp. 1539-1549, May 2015.
- [4] G. He, S. Dong, J. Qi, and Y. Wang, "Robust state estimator based on maximum normal measurement rate," *IEEE Trans. Power Syst.*, vol. 26, no. 4, pp. 2058-2065, Nov. 2011.
- [5] J. Zhao, "Dynamic state estimation with model uncertainties using H_∞ extended Kalman filter," *IEEE Trans. Power Syst.*, vol. 33, no. 1, pp. 1099-1100, Jan. 2018.
- [6] A. Rouhani and A. Abur, "Constrained iterated unscented Kalman filter for dynamic state and parameter estimation," *IEEE Trans. Power Syst.*, vol. 33, no. 3, pp. 2404-2414, May 2018.
- [7] Y. Wang, Z. Yang, Y. Wang, V. Dinavahi, J. Liang, and K. Wang, "Robust dynamic state estimation for power system based on adaptive cubature Kalman filter with generalized coreentropy loss," *IEEE Trans. Instrum. Meas.*, DOI: 10.1109/TIM.2022.3175025, 2022.
- [8] N. Zhou, D. Meng, Z. Huang, and G. Welch, "Dynamic state estimation of a synchronous machine using PMU data-A comparative study," *IEEE Trans. Smart Grid*, vol. 6, no. 1, pp. 450-460, Jan. 2015.
- [9] E. Ghahremani and I. Kamwa, "Local and wide-area PMU-based decentralized dynamic state estimation in multi-machine power systems," *IEEE Trans. Power Syst.*, vol. 31, no. 1, pp. 547-562, Jan. 2016.
- [10] J. Zhao, M. Netto, and L. Mili, "A robust iterated extended Kalman filter for power system dynamic state estimation," *IEEE Trans. Power Syst.*, vol. 32, no. 4, pp. 3205-3216, Jul. 2017.
- [11] S. Akhlaghi, N. Zhou, and Z. Huang, "A multi-step adaptive interpolation approach to mitigating the impact of nonlinearity on dynamic state estimation," *IEEE Trans. Smart Grid*, vol. 9, no. 4, pp. 3102-3111, Jul. 2018.
- [12] S. Wang, W. Gao, and A. Meliopoulos, "An alternative method for power system dynamic state estimation based on unscented transform," *IEEE Trans. Power Syst.*, vol. 27, no. 2, pp. 942-950, May 2012.
- [13] J. Qi, K. Sun, J. Wang, H. Liu, "Dynamic state estimation for multi-machine power system by unscented Kalman filter with enhanced numerical stability," *IEEE Trans. Smart Grid*, vol. 9, no. 2, pp. 1184-1196, Mar. 2018.
- [14] J. Zhao and L. Mili, "Robust unscented Kalman filter for power system dynamic state estimation with unknown noise statistics," *IEEE Trans. Smart Grid*, vol. 10, no. 2, pp. 1215-1224, Mar. 2019.
- [15] Y. Wang, Y. Sun, V. Dinavahi, K. Wang and D. Nan, "Robust dynamic state estimation of power systems with model uncertainties based on adaptive unscented H-infinity filter," *IET Gener. Transm. Distrib.*, vol. 13, no. 12, pp. 2455-2463, Jun. 2019.
- [16] A. Sharma, S. C. Srivastava, and S. Chakrabarti, "A cubature Kalman filter based power system dynamic state estimator," *IEEE Trans. Instrum. Meas.*, vol. 66, no. 8, pp. 2306-2045, Aug. 2017.
- [17] M. Amin Kardan, M. Asemiani, A. Khayatian, N. Vafamand, M. Khooban, and F. Blaabjer, "Improved stabilization of nonlinear DC microgrids: cubature Kalman filter approach," *IEEE Trans. Ind. Appl.*, vol. 54, no. 5, pp. 5104-5112, Sep. 2018.
- [18] W. Rosenthal, A. Tartakovskiy, Z. Huang, "Ensemble Kalman filter for dynamic state estimation of power grids stochastically driven by time-correlated mechanical input power," *IEEE Trans. Power Syst.*, vol. 33, no. 4, pp. 3701-3710, Jul. 2018.

- [19] Y. Cui and R. Kavasseri, "A particle filter for dynamic state estimation in multi-machine systems with detailed models," *IEEE Trans. Power Syst.*, vol. 30, no. 6, pp. 3377-3385, Nov. 2015.
- [20] Y. Yu, Z. Wang, and C. Lu, "A joint filter approach for reliable power system state estimation," *IEEE Trans. Instrum. Meas.*, vol. 68, no. 1, pp. 87-94, Jan. 2019.
- [21] Y. Cui, R. G. Kavasseri, and S. M. Brahma, "Dynamic state estimation assisted out-of-step detection for generators using angular difference," *IEEE Trans. Power Del.*, vol. 32, no. 3, pp. 1441-1449, Jun. 2017.
- [22] Y. Liu, A. Meliopoulos, R. Fan, L. Sun, and Zhenyu Tan, "Dynamic state estimation based protection on series compensated transmission lines," *IEEE Trans. Power Del.*, vol. 32, no. 5, pp. 2199-2209, Oct. 2017.
- [23] X. Wang and E. E. Yaz, "Stochastically resilient extended Kalman filtering for discrete-time nonlinear systems with sensor failures," *Int. J. Syst. Sci.*, vol. 1, no. 9, pp. 1393-1401, Jan. 2014.
- [24] Y. Sun, Y. Wang, X. Wu, and Y. Hu, "Robust extended fractional Kalman filter for nonlinear fractional systems with missing measurements," *J. Frankl. Inst.*, vol. 355, pp. 361-380, Jan. 2018.
- [25] S. Deshmukh, N. Balasubramaniam and A. Pahwa, "State estimation and voltage/VAR control in distribution network with intermittent measurements," *IEEE Trans. Smart Grid*, vol. 5, no. 1, pp. 200-209, Jan. 2014.
- [26] L. Hu, Z. Wang, I. Rahman, and X. Liu, "A constrained optimization approach to dynamic state estimation for power systems including PMU and missing measurements," *IEEE Trans. Control Syst. Technol.*, vol. 24, no. 2, pp. 703-710, Jan. 2016.
- [27] X. Wang and E. Yaz, "Smart power grid synchronization with fault tolerant nonlinear estimation," *IEEE Trans. Power Syst.*, vol. 31, no. 6, pp. 4806-4816, Oct. 2016.
- [28] Y. Wang, Y. Sun, Z. Wei, and G. Sun, "Parameters estimation of electromechanical oscillation with incomplete measurement information," *IEEE Trans. Power Syst.*, vol. 33, no. 5, pp. 5016-5028, Sep. 2018.
- [29] J. Hu, Z. Wang, H. Gao, and L. Stergioulas, "Extended Kalman filtering with stochastic nonlinearities and multiple missing measurements," *Automatica*, vol. 48, no. 9, pp. 2007-2015, Sep. 2012.
- [30] H. Yuan and X. Song, "A modified EKF for vehicle state estimation with partial missing measurements," *IEEE Signal Process. Lett.*, vol. 29, pp. 1594-1598, Mar. 2022.
- [31] K. Horiguchi, T. Iikubo, Y. Beppu, Y. Hyakutake, and O. Sugihara, "Low-attenuation variable mode control using twist processing for step-index optical fiber loops," *IEEE Photon. Technol. Lett.*, vol. 29, pp. 1594-1598, Aug. 2019.
- [32] P. Anderson and A. A. Faud, *Power System Control and Stability*. IAAMES: Iowa State University, 1977.
- [33] T. Mori, N. Fukuma, and M. Kuwahara, "Explicit solution and eigenvalue bounds in the Lyapunov matrix equation," *IEEE Trans. Autom. Control*, vol. AC-31, no. 7, pp. 656-658, Jul. 1986.
- [34] D. Simon, *Optimal State Estimation Kalman, H ∞ , and Nonlinear Approaches*. Hoboken, NJ, USA: Wiley, 2006.
- [35] J. Hartikainen, A. Solin, and S. Särkkä, "Optimal filtering with Kalman filters and smoothers," Dept. of Biomedical Engineering and Computational Sciences, Aalto University School of Science, Aug. 2011.
- [36] D. Y. Wong, G. J. Rogers, B. Porretta, and P. Kundur, "Eigenvalue analysis of very large power systems," *IEEE Trans. Power Syst.*, vol. 3, no. 2, pp. 472-480, May 1988.
- [37] A. K. Singh and B. C. Pal, "Decentralized dynamic state estimation in power systems using unscented transformation," *IEEE Trans. Power Syst.*, vol. 29, no. 2, pp. 794-804, Mar. 2014.
- [38] J. Chow and G. Rogers, User manual for power system toolbox, Version 3.0, 1991-2008.



Yi Wang (M'20) received his B.S. degree from Luoyang Institute of Science and Technology, Luoyang, China, in 2014; and received his Ph.D. degrees from Hohai University, Nanjing, China, in 2020. He was a visiting scholar at the University of Alberta between 2018 and 2019.

He is currently a lecturer at Zhengzhou University. His current research interests include theoretical and algorithmic studies in power system estimation, parameters identification, power system dynamics, signal processing, cyber security, optimal planning

and operation of integrated energy system. He is also an active reviewer for many international journals.



Yaoqiang Wang (M'16-SM'21) received his B.S. degree from Hangzhou Dianzi University, Hangzhou, China, in 2006; and his M.S. and Ph.D. degrees from the Harbin Institute of Technology, Harbin, China, in 2008 and 2013, respectively.

He is currently a Professor with the School of Electrical and Information Engineering, Zhengzhou University, Zhengzhou, China. He is also serving as the Director of the Henan Provincial Engineering Research Center of Power Electronics and Energy Systems (HERC-PEES). He has authored more than 60 technical papers including over 50 journal papers, and is the holder of more than 20 patents. His current research interests include power electronics and electrical drives, renewable power generation, new energy power system, power system operation and control.



Yonghui Sun (M'16) received the Ph.D. degree from the City University of Hong Kong, Hong Kong, in 2010.

He is currently a Professor with the College of Energy and Electrical Engineering, Hohai University, Nanjing, China. He has authored more than 100 papers in refereed international journals. His research interests include stability analysis and control of power systems, optimal planning and operation of integrated energy system, optimization algorithms, and data analysis. Dr. Sun was the recipient of the

First Award of Jiangsu Provincial Progress in Science and Technology in 2010 as the Fourth Project Member. He is an active reviewer for many international journals.



Venkata Dinavahi (M'00-SM'08-F'19) received the B.Eng. degree in Electrical Engineering from Visvesvaraya National Institute of Technology (VNIT), Nagpur, India, in 1993, the M.Tech. degree in Electrical Engineering from the Indian Institute of Technology (IIT) Kanpur, India, in 1996, and the Ph.D. degree in Electrical and Computer Engineering from the University of Toronto, Ontario, Canada, in 2000.

He is currently a Professor in Energy Systems within the Department of Electrical and Computer Engineering, University of Alberta, Edmonton, Alberta, Canada. He is a Fellow of the Engineering Institute of Canada (EIC) and a Fellow of the Asia-Pacific Artificial Intelligence Association (AAIA). His research interests include real-time simulation of large-scale power systems and power electronic systems, electromagnetic transients, device-level modeling, machine learning, artificial intelligence, and parallel and distributed computing. He is a Professional Engineer in the Province of Alberta, Canada.



Jun Liang (M'02-SM'12) received his B.S. degree in Electric Power System and its Automation from the Huazhong University of Science and Technology, Wuhan, China, in 1992; and his M.S. and Ph.D. degrees in Electric Power System and its Automation from the China Electric Power Research Institute (CEPRI), Beijing, in 1995 and 1998, respectively.

Prof. Liang is a Fellow of the Institution of Engineering and Technology (IET). He is the Chair of IEEE UK and Ireland Power Electronics Chapter. He is an Editorial Board Member of CSEE JPES.

He is an Editor of the IEEE Transactions on Sustainable Energy.



Kewen Wang (M'06) received the B.S. degree from the Zhengzhou Institute of Technology, Zhengzhou, China, in 1985, the M.S. degree from Tianjin University, Tianjin, China, in 1988, and the Ph.D. degree from The Hong Kong Polytechnic University, Hong Kong, SAR, China, in 2000.

He is currently a Professor with the School of Electrical Engineering, Zhengzhou University, Zhengzhou. His research interests include power electronics, renewable power generation, power system stability analysis and control, and reactive power

optimization.